Water-soluble binders for MCMB carbon anodes for lithium-ion batteries

Fabrice M. Courtel, Svetlana Niketic, Dominique Duguay, Yaser Abu-Lebdeh*, Isobel J. Davidson

National Research Council Canada, 1200 Montreal Road, Ottawa, Ontario, K1A 0R6 Canada

ABSTRACT

We have investigated the suitability of four different binders for the conventional mesocarbon microbeads (MCMBs) anode material in Li-ion batteries. Unlike the conventional polyvinylidene fluoride (PVDF), the binders were water soluble and were either cellulose based, such as the lithium and sodium salts of carboxymethyl cellulose (NaCMC, and LiCMC) and Xanthan Gum (XG), or the conjugated polymer: poly(3,4-ethylendioxythiophene) (PEDOT, a.k.a. Baytron). All binders were commercially available except LiCMC, which was synthesized and characterized by FTIR and NMR. Thermal studies of the binders by TGA and DSC showed that, in air, the binders have a broad melting event at 100–150 °C, with an onset temperature for decomposition above 220 °C. Li/MCMB half-cell batteries were assembled using the studied binders. Slow scan voltammograms of all cells showed characteristic lithium insertion and de-insertion peaks including that of the SEI formation which was found to be embedded into the insertion peaks during the first cycle. Cycling of the cells showed that the one containing XG binder gave the highest capacities reaching 350 mAh g^{-1} after 100 cycles at C/12, while the others gave comparable capacities to those of the conventional binder PVDF. The rate capabilities of cells were examined and found to perform well up to the studied C/2 rate with more than 50% capacity retained. Further studies of the XG-based MCMB electrodes were performed and concluded that an optimal thickness of 300–365 μm gave the highest capacities and sustained high C-rates.

Crown Copyright © 2010 Published by Elsevier B.V. All rights reserved.

1. Introduction

Carbon has been widely used as an anode material in commercial Li-ion batteries since 1991 when Sony Corporation launched its first rechargeable Li-ion battery (carbon/LiCoO$_2$) [1]. The layered allotrope of carbon, graphite, is used in particular due to: (i) its high electronic conductivity (10^3 to 10^4 S cm^{-1}), (ii) its low cost, (iii) its good capacity retention, and (iv) more importantly its long cycle life. In the 1970s, Hérold et al. reported the chemical formation of a lithiated carbon graphite (LiC$_6$) [2–4], which was later demonstrated to be electrochemically viable and reversible [5,6] and soon after it was adopted in Li-ion batteries. A maximum of one lithium for six carbons can be intercalated between the graphene layers of graphite. The theoretical gravimetric specific capacity of carbon graphite is 372 mAh g^{-1} and for its volumetric is 830 mAh ml^{-3} (calculated using carbon as a starting material [7]). When lithium ions are intercalated in graphite, the distance between the graphene layers increases from 0.335 nm to 0.372 nm [1,8,9], which corresponds to a volume change of about 10% in the direction normal to the plane [10]. Thus it allows the use of polyvinylidene fluoride

(PVDF) as a binder that can be elongated to about 20% of its length before breaking [10].

Binders are an important part of electrode formulation because they maintain the physical structure of the electrode; without a binder the electrode would fall apart. PVDF continues to be successfully used in commercial Li-ion batteries as it exhibits excellent properties. It does not get reduced at low potential (5 mV versus Li/Li$^+$) nor oxidized at high potential (5 V versus Li/Li$^+$) at room temperature, but has the following shortcomings:

(1) At elevated temperatures, it has been reported that PVDF reacts with lithium metal and LiC$_6$ to form LiF and some –(–C=C–F)– species via an exothermic reaction which causes a risk for the onset of thermal runaway [11–13]. To avoid this risk, research is currently focused on finding alternative non-fluorinated binders [14–18]. Even though they were still insoluble in water, Maleki et al. [13] and Du Pasquier et al. [11] showed that reduced heat was obtained when poly(phenol-formaldehyde), poly(vinylchloride) or poly(acrylonitrile) were used as binders.
(2) Another disadvantage of using PVDF is its price which is about US$ 20 per kg in North America (€15–18 per kg in Europe [19]).
(3) PVDF requires the use of non-environmentally friendly solvents to cast the electrode formulation, such as N-methyl-2-pyrrolidone (NMP). According to its material safety data sheet,

it is a known mutagen, tumorigen and reproductive effector; its LD_{50} on skin rabbit is 8 mg kg^{-1}.

(4) In addition, as mentioned by Lux et al. it is not easy to dispose PVDF at the end of the battery life [19]. Thus binders with decomposition products that are more environmentally friendly are needed for preparing electrodes materials for Li-ion batteries.

Water is very attractive as an alternative to organic solvents and water-soluble binders have already been studied with silicon and tin anode materials, where more flexible and compatible binders are needed. Upon cycling, these active materials suffer from large volume changes between the charge and the discharge states (250–300% [1]). Consequently PVDF cannot be used because it is not able to accommodate large volume changes. Binders such as styrene-butadiene rubber (SBR), sodium carboxymethyl cellulose (NaCMC), and combinations of both were studied with silicon and provided improved capacity retention [20–23]. NaCMC has also been successfully used as a binder with $Li_4Ti_5O_{12}$ [24], $LiFePO_4$ [19,24], and commercial SnO_2 nanoparticles [25]. In addition to being able to accommodate the volume change during cycling, it has the advantage of being water soluble because of the carboxymethyl groups attached to cellulose. As mentioned by Lux et al., the use of NaCMC has the advantage of rendering the recycling of Li-ion battery anodes easier [19] and friendlier to the environment, as it was demonstrated that calcination of NaCMC at 700 °C yields Na_2CO_3, a naturally occurring mineral deposit [26,27]. In addition, the price of NaCMC is much lower than PVDF, about US$ 6 per kg in North America (€1–2 per kg in Europe [19]) since NaCMC is widely used in the food industry as a thickener. Finally, the performance of NaCMC has already been investigated with natural carbon graphite by Hochgatterer et al. [22], obtaining a capacity very close to that obtained with PVDF. Drofenik et al. also investigated the use of NaCMC with natural graphite and obtained a capacity of 325 mAh g^{-1} after 10 cycles [28]. Other water-soluble binders have been reported for carbon graphite, such as poly(acrylamide-co-diallyldimethylammonium chloride) (PAMAC) [29] and gelatine [30], and capacities similar to those obtained with PVDF were reported.

Herein we report the use of water-soluble binders as alternatives to the well-known PVDF/NMP couple. Mesocarbon microbeads (MCMB) was used as the anode material in this study as it regularly shows good performance thanks to its high packing density and narrow particle size distribution, ranging from 1 to 44 μm. MCMB exhibits good capacity retention and rate capabilities due to edge-plane surfaces [31–34]. We first studied two cellulose-based salts: (i) NaCMC obtained from two different suppliers showing different viscosities and performance, and (ii) lithium carboxymethyl cellulose (LiCMC) synthesized and characterized in-house. We also investigated another cellulose-based binder, Xanthan Gum (XG), which is also water-soluble and used widely as a food thickener. XG is more cost effective than PVDF, about US$ 13 per kg in North America. We also investigated the use of poly(3,4-ethylendioxythiophene) which has the advantage of being electronically conductive (10–500 mS cm^{-1}) [35,36] but is quite expensive.

2. Experimental

MCMB carbon graphite (Nippon Carbon Co. Ltd) was used as received and stored at 90 °C before use. As previously mentioned, five different binders were investigated: (i) the conventional polyvinylidene fluoride (PVDF, Kynarflex2800) 3 wt% dissolved in N-methyl-2-pyrrolidone (NMP, Sigma–Aldrich, anhydrous, 99.5%), (ii) sodium carboxymethyl cellulose (NaCMC) obtained from two

suppliers Calbiochem (viscosity 42.0 mPa s) and Sigma–Aldrich (average Mw ∼ 90,000, degree of substitution 0.70) used as a 5 wt% aqueous solution, (iii) lithium carboxymethyl cellulose (LiCMC) synthesized and characterized in-house, used as a 2.5 wt% aqueous solution, (iv) xanthan gum (XG, Jungbunzlauer, Na was the counter ion) 1 wt% in water, and (v) poly(3,4-ethylendioxythiophene) with polystyrenesulfonate as a counter ion (a.k.a. PEDOT/PSS or Baytron®, Sigma–Aldrich) obtained as a 1.5 wt% aqueous solution.

LiCMC was synthesized in-house following a modified reported procedure [26]. At room temperature, 1 g of cellulose (Sigma–Aldrich, α-cellulose) was suspended in 35 ml i-propanol (EMD) and 13 ml of double distilled H_2O. While the solution was stirring, 3.5 g of LiOH·H_2O (Anachemia, 98%) was added over 10 min. The solution was stirred overnight after which a solution of monochloroacetic acid (Sigma–Aldrich, 99+%), made of 3 g in 4 ml i-propanol, was added dropwise. The solution was heated at 55 °C in air under reflux for 5 h and then cooled to room temperature. An unexpected gummy solid resulted which was not obtained in reference [26]. The gummy solid was filtered, washed with double distilled H_2O, and then dissolved in 100 ml H_2O and stirred overnight. The solution was neutralized with acetic acid (FisherBrand, ACS grade) and filtered in order to remove some insoluble particles (most probably unreacted cellulose). LiCMC was precipitated by adding large quantities of i-propanol (600 ml). Upon stirring, (about 1 h) a white fluffy precipitate formed. The product was then filtered and dried at 55 °C overnight producing 1.04 g of white powder.

Thermogravimetric analyses (TGA) were performed using platinum pans in order to characterize the binders' thermal stability (Hi-Res TGA 2950 TA instrument). The binders were first dried for a few days at 55 °C and then heated at 5 °C min^{-1} up to 600 °C in air. Differential scanning calorimetric (DSC) analysis was performed using a TA Instruments 2920. Samples were prepared in unsealed aluminum pans and then scanned from room temperature to the onset decomposition temperature at 10 °C min^{-1} rate. Fourier-transform infrared spectroscopy (FTIR) in attenuated total reflectance (ATR) mode was performed on the cellulose-based binders using a ZnSe crystal plate (Bruker Tensor IFS 66/S). NMR spectra were obtained for the carboxymethyl cellulose binders using a Varian Unity Inova 400 MHz instrument (probe: 5 mm broadband).

Cyclic voltammetry and cell cycling were carried out on half-cells using 2325-type coin cells assembled in an argon-filled glove box. Cyclic voltammograms were recorded using a BioLogic VMP3 potentiostat. The cyclic voltammograms were recorded between 0.005 V and 1.5 V versus Li/Li$^+$ at a scan rate of 0.1 mV s^{-1}. Capacity measurements were performed by galvanostatic experiments carried out on a multichannel Arbin battery cycler. The working electrode was first charged (lithiated) down to 5 mV versus Li/Li$^+$ at different C-rates and then discharged (delithiated) up to 1.5 V versus Li/Li$^+$. The mass of active material used in the calculation is the mass of the carbon graphite (MCMB).

The working electrodes were prepared as follows: MCMB was mixed with 5 wt% Super carbon (Timcal) and 10 wt% binder. The electrode films were made by spreading onto a high purity copper foil current collector (cleaned using a 2.5% HCl solution in order to remove the copper oxide layer) using an automated doctor-blade and then dried overnight at 85 °C in a convection oven. Individual disk electrodes (∅ = 12.5 mm) were punched out, dried at 80 °C under vacuum overnight and then pressed under a pressure of 0.5 metric ton. A lithium metal disk (∅ = 16.5 mm) was used as a negative electrode (counter electrode and reference electrode). 70 μL of a solution of 1M LiPF$_6$ in ethylene carbonate/dimethyl carbonate (EC:DMC, 1:1, v/v) was employed as electrolyte and spread over a double layer of microporous propylene separators (Celgard 2500,
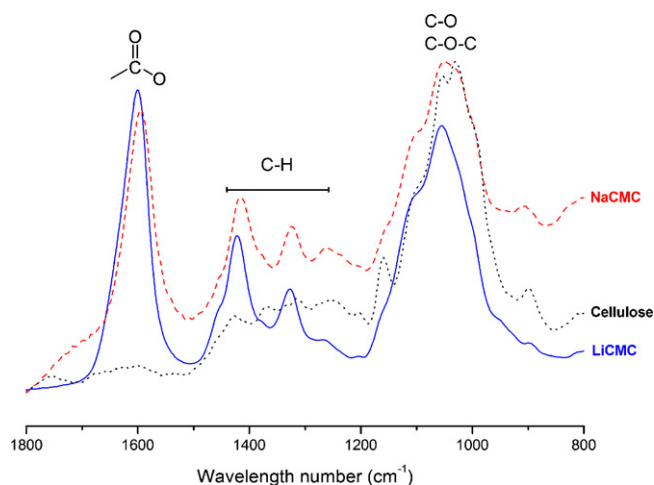
Fig. 1. FTIR spectra of cellulose, NaCMC and LiCMC.

30 μm thick, Ø = 2.1 mm). The cells were assembled in an argon-filled dry glove box at room temperature.

3. Results and discussion

3.1. Synthesis and characterization of LiCMC

Unlike other binders investigated in this study, LiCMC was not commercially available and was synthesized according to the synthesis described in the experimental section. The as-synthesized LiCMC powder was analysed by FTIR, ^{1}H NMR, and ^{13}C NMR in order to verify that the carboxymethyl group has bonded to the cellulose.

Fig. 1 shows the FTIR spectra of the cellulose, the commercial NaCMC (Calbiochem), and the synthesized LiCMC. Both NaCMC and LiCMC spectra show the presence of an extra vibrational band at 1650–1550 cm^{-1} which corresponds to the carboxylic functional group that is absent in the FTIR spectra of cellulose. In addition, the FTIR analysis also showed the presence of C-H stretching of methyl groups attached to the carboxylic group between 1420 and 1260 cm^{-1}. Vibrational bands between 900 and 1100 cm^{-1} are attributed to the ether groups from the cellulose.

The LiCMC powder was also characterized by ^{1}H NMR and ^{13}C NMR. The ^{1}H NMR spectra showed peaks at: δ 3.35 (s, CH), δ 3.50 (s, CH), δ 3.79 (s, CH), δ 3.80–4.05 (m, CH, CH$_2$), δ 4.25 (m, CH), and δ 4.36 (m, CH). The different carbons of the LiCMC formula have been
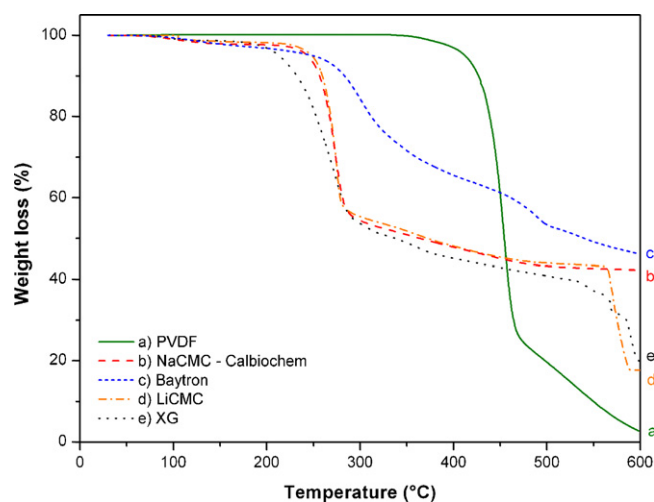

Fig. 3. TGA graph of the PVDF, NaCMC (Calbiochem), LiCMC, Baytron and XG.

identified with numbers in Fig. 2. ^{13}C NMR spectra, also in Fig. 2, showed peaks at δ 60.39 corresponding to C$_6$. The multiplet from δ 69.10 to δ 78.82 belongs to the three following carbons: C$_2$, C$_3$ and C$_5$. The peak at δ 82.44 corresponds to C$_4$ and the peak at δ 102.71 belongs to C$_1$. More importantly, the ^{13}C NMR peak that appeared at δ 178.13 corresponds to the COO– group [26,37] and thus confirms that the LiCMC has been successfully synthesized. For comparison purposes, NaCMC (Calbiochem) was also analysed by ^{1}H NMR and ^{13}C NMR and the same peaks were observed.

3.2. Thermal stability of the binders

The thermal stability of the different binders was measured by TGA and DSC; the scans are shown in Figs. 3 and 4, respectively. Even though the binders were kept at 50 °C for a few days, TGA results (except for PVDF) showed a first 1.5–2.5 wt% weight loss step at 150 °C due to loss of water. Thus all binders are stable in the temperature range used for the preparation and drying of the electrodes, i.e. 20–90 °C. XG is the first binder to show decomposition which starts at about 200 °C, followed by NaCMC and LiCMC at 250 °C, as already reported [26,27]. LiCMC and NaCMC show exactly the same decomposition pattern up to 550 °C with a weight loss of about 43 wt% at 300 °C and an additional 12 wt% loss at 550 °C. Baytron started decomposing at a higher temperature of 275 °C but this was followed by a two-step weight loss of 50 wt% at 600 °C.
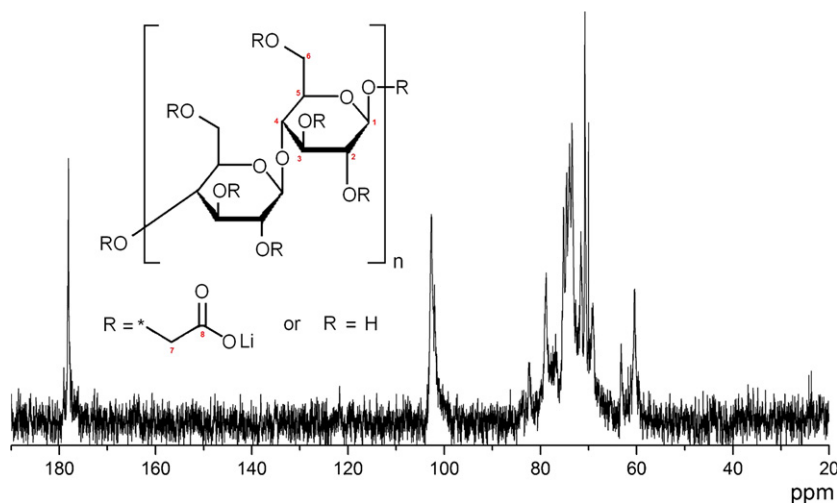

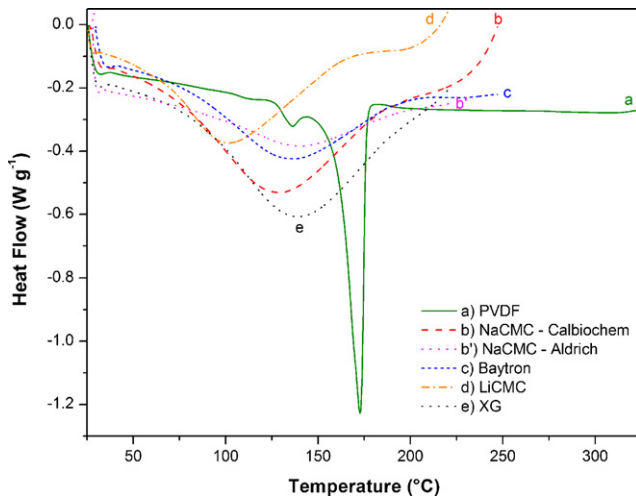**Fig. 2.** ^{13}C NMR spectra of LiCMC and LiCMC formula.

Fig. 4. DSC graph of PVDF, NaCMCs, LiCMC, Baytron and XG.

PVDF showed an onset temperature of about 400 °C with a rapid decomposition associated with a weight loss of about 75 wt% at 450 °C followed by another 20 wt% up to 600 °C. TGA showed that the binders are stable in the temperature range that was used for preparing and drying the electrodes.

DSC measurements were performed to identify changes in the state of the different binders before decomposition. As shown in Fig. 4, the different state changes occur at different temperatures. NaCMCs, Baytron, and XG all show a broad endothermic transition peak at 140–145 °C whereas LiCMC shows a transition peak at a lower temperature, 100 °C. These large endothermic transition peaks are due to the melting of the amorphous state of these binders. PVDF being more crystalline shows a first transition at 140 °C and a melting temperature of 175 °C.

3.3. Cyclic voltammetry

Fig. 5 shows CVs of the MCMB electrodes prepared using the 5 different binders. The batteries were first cycled from the open circuit potential (OCP usually c.a. 2.7–3 V versus Li/Li$^+$) and 0.005 V and then between 0.005 V and 1.5 V versus Li/Li$^+$. As expected, the use of PVDF provides a well-identified peak at 0.65 V which correspond to the SEI formation that fully disappears on the second cathodic sweep [38]. NaCMC (Calbiochem) exhibit a few reduc-
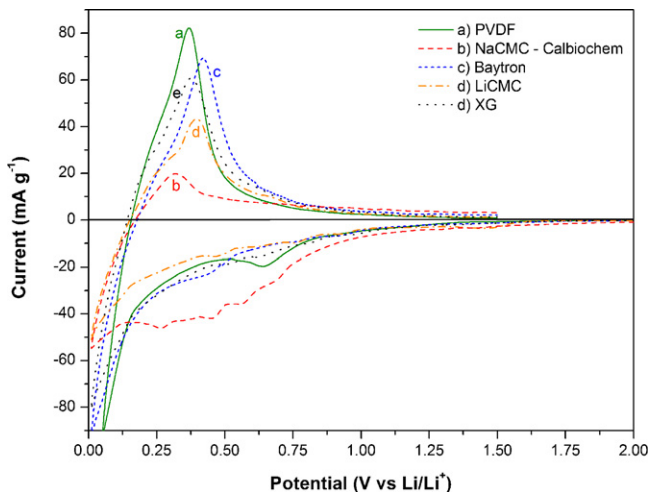
tion peaks ranging from 0.75 V to 0.25 V and from 1 V to 0.5 V in the case of LiCMC and XG; these peaks correspond most probably to the SEI formation since they do not appear for subsequent cycles. In the case of Baytron, the SEI formation occurs at about 0.5 V. The CV for NaCMC (Sigma–Aldrich) is not shown because the currents were too low to compare to the other binders, and no useful information could be inferred. The second reduction process (close to 0 V) corresponds to lithium insertion into carbon graphite (Li$_x$C$_6$, $x \leq 1$). The oxidation reaction peaks that appear between 0.3 V and 0.4 V correspond to lithium de-insertion from Li$_x$C$_6$. The position of the lithium de-insertion is slightly shifted depending on the nature of the binder used. The use of NaCMC (Calbiochem) provided a lithium de-insertion potential of about 0.32 V, 0.36 V for PVDF, 0.37 V for XG, 0.40 V for LiCMC, and 0.42 V for Baytron. Because the MCMB particles are coated with an organic layer made mostly of the binder, it is expected that the nature of the binder is going to enhance the electrode/electrolyte interface. The binder adds a physical barrier to lithium insertion/de-insertion, which makes the lithium ion movement process more difficult than in the bare binder. For example, Baytron, which is an electronic conductor but an non-ionic conductor showed the more positive shift, which makes the de-insertion more difficult. On the opposite, the cellulose-based binders (NaCMC, LiCMC and XG) are electronic insulators, but expected to be ionically more conductive than Baytron, showed negative shifts of the lithium de-insertion. In Fig. 6 one can find the 1st and the 5th cyclic voltammograms of each electrode prepared using the different binders. All CVs clearly show a difference between the 1st and the 5th cycle, specifically the reduction process that corresponds to the SEI formation that is expected to disappear in the 5th cycle.

3.4. Battery cycling

Fig. 7 shows the 1st charge–discharge profile of the electrodes prepared using the different binders. As already shown by the CV measurements, the electrode made using PVDF shows the formation of the SEI at about 0.65 V, and then it showed the expected characteristic plateau for lithium insertion between 0.1 and 0.05 V. This electrode has a first discharge capacity of 375 mAh g^{-1}. Baytron, NaCMC (Calbiochem) and XG show the same first discharge capacity values as PVDF. As already observed with the CV measurements, in the case of NaCMC (Calbiochem) the SEI formation is very different from the other binders. A large slope between 0.75 V and 0.1 V is observed before lithium insertion into graphite. When the NaCMC (Sigma–Aldrich) is used, it was not possible to obtain a capacity over 25 mAh g^{-1} for the first discharge. All batteries showed an irreversible capacity between the 1st discharge and the 1st charge, which represents a capacity loss due, to the SEI formation being: 10.7% for PVDF, 28.0% for NaCMC (Calbiochem), 28.4% for Baytron, 6.7% for LiCMC and only 6.7% for XG.

Fig. 8 shows the cycling behaviour of MCMB anodes at C/12 over 100 cycles. As expected, PVDF that was used as a reference provided a first discharge capacity of 375 mAh g^{-1} and a stable reversible capacity of 337 mAh g^{-1} after 100 cycles. Fig. 8 also shows the performance of the two NaCMCs which do not exhibit the same behaviour. When NaCMC (Sigma–Aldrich) is used, almost no capacity is obtained for the first few cycles and then the capacity increased exponentially up to 260 mAh g^{-1}. On the other hand, NaCMC (Calbiochem) showed a better performance with a first discharge capacity of about 375 mAh g^{-1} and a stable reversible capacity of 310 mAh g^{-1} after 100 cycles which is similar to what Drofenik et al. obtained [28]. LiCMC showed a first discharge capacity of about 290 mAh g^{-1}, which is lower than most binders; however, upon cycling, a stable reversible capacity of about 300 mAh g^{-1} was obtained. Baytron, which has the advantage of being electronically conductive, showed a first discharge capac-

Fig. 5. Cyclic voltammetry of MCMB anodes prepared using different binders: (a) PVDF, (b) NaCMC – Calbiochem, (c) Baytron, (d) LiCMC, and (e) XG.
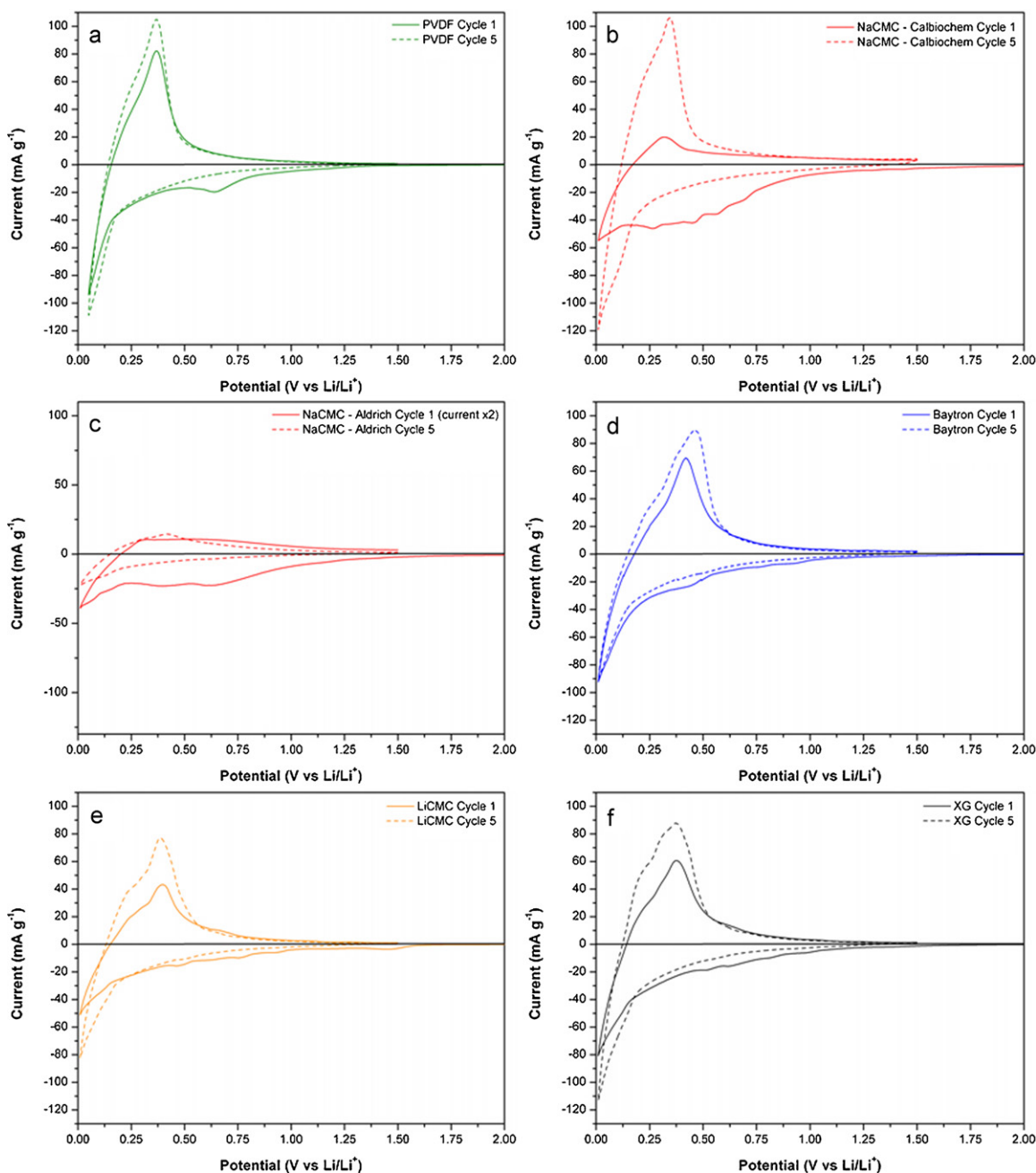
Fig. 6. Cyclic voltammograms, cycle #1 and cycle #5, of MCMB anodes prepared using different binders: (a) PVDF, (b) NaCMC – Aldrich, (c) NaCMC – Calbiochem, (d) Baytron, (e) LiCMC, and (f) XG.

ity of about 375 mAh g^{-1} and a reversible one of 330 mAh g^{-1} after 100 cycles. Surprisingly enough, Baytron showed very good stability at low potentials. It is known that polymers undergo n-doping at low potential that is not sustained upon cycling due to the inability of the conjugated chain to bear the negative change [39]. The last and most interesting binder is XG. It also provided a first discharge capacity of about 375 mAh g^{-1}, and a stable reversible capacity of 350 mAh g^{-1} after 100 cycles.

Unlike Hochgatterer et al. [22], with NaCMC as a binder in our case, it has not been possible to obtain a capacity value that was as good as the one with PVDF. The performance of NaCMC usually depends on the supplier, the degree of substitution (DS), and the length of the polymer chain. The DS indicates the average number of carboxymethyl groups attached to the glucose unit. A low DS usually provides better performance because of additional interac-

tions between NaCMC and graphite [40]. For this study, it has been decided to use NaCMCs with a low degree of substitution, ranging from 0.7 to 0.8. NaCMC provided by Sigma–Aldrich had a DS of 0.7 whereas NaCMC provided by Calbiochem had a DS of 0.8. Even though these values are very close, the viscosity measured for a 2 wt% aqueous solution provided different values: 28 cP for NaCMC (Sigma–Aldrich) and 50 cP for NaCMC (Calbiochem). The chain length (molecular weight) was not available for NaCMC (Calbiochem), but one can assume that it is longer due to the higher viscosity value, which can also be explained by the presence of strong ionic interactions and entanglements among the chains.

The rate capability of these anodes was also investigated and the results are shown in Fig. 9. The batteries were cycled five times at each C-rate: C/12, C/9, C/6, C/3, C/2, C, 2C and then back at C/12. As shown in Fig. 9, at C/12 XG shows the highest discharge capac-
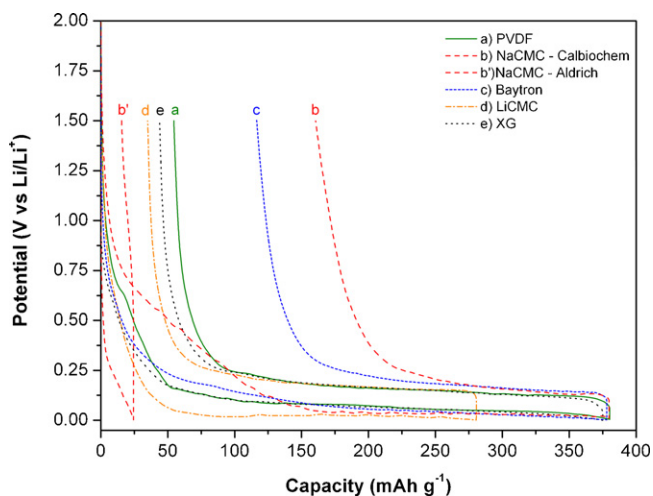
Fig. 7. 1st Charge–discharge profiles of the MCMB electrodes prepared with the different binders and cycled at C/12 between the OCP and 5 mV, and then between 5 mV and 1.5 V versus Li/Li⁺.
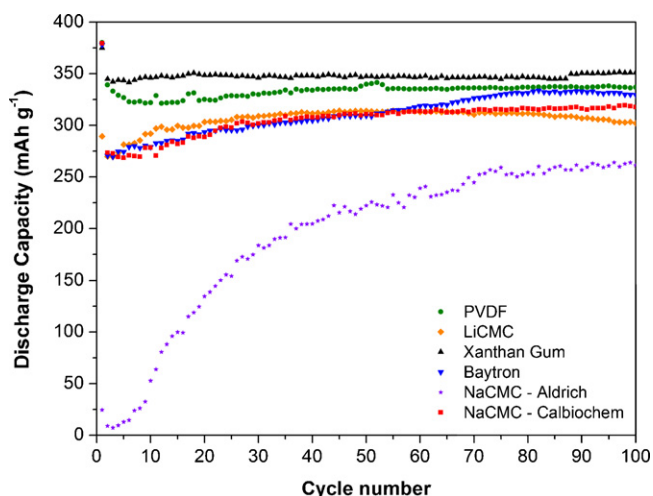

Fig. 8. Cycling behaviour of MCMB anodes prepared with different binders, cycled between 5 mV and 1.5 V versus Li/Li⁺ at C/12.
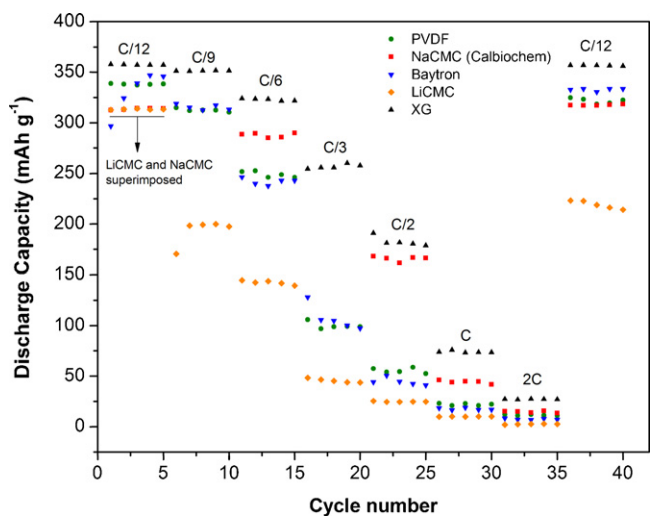

Fig. 9. Cycling behaviour of MCMB anodes prepared with different binders, cycled between 5 mV and 1.5 V versus Li/Li⁺ at different C-rates C/12, C/9, C/6, C/3, C/2, C, 2C and back to C/12.

ity values of 356 mAh g⁻¹, followed by Baytron, PVDF, NaCMC and finally LiCMC which showed capacities of 310 mAh g⁻¹. By increasing the C-rate up to C/2, XG still shows a capacity of 180 mAh g⁻¹ which represents 51% of the capacity obtained at C/12. At C/2, NaCMC (Calbiochem) shows a capacity of 165 mAh g⁻¹ (53% of the capacity at C/12). The three other binders showed capacities around 50 mAh g⁻¹. At C, capacities drastically decreased down to 73 mAh g⁻¹ for XG which represents 21% of the capacity observed at C/12, and down to 45 mAh g⁻¹ for NaCMC which represents 14% of the capacity observed at C/12. When the batteries were cycled back at C/12, the ones prepared with NaCMC and XG showed a total recovery of the capacity: 357 mAh g⁻¹ and 316 mAh g⁻¹, respectively. However, Baytron and PVDF showed a slight capacity loss of 4%. In the case of LiCMC, a large capacity loss of 30% is observed, probably due to a degradation of LiCMC or its involvement in surface reactions at higher C-rates.

When comparing our best data with those reported by Guidotti et al., the capacity values that we obtained at C/12 and C/6 were higher [41] In both cases carbon MCMB and the same cycling procedure were used but with 15 wt% of PVDF as a binder [41] At C/12 capacities obtained were 325 mAh g⁻¹ and 375 mAh g⁻¹, while at C/6 they were 300 mAh g⁻¹ and 325 mAh g⁻¹, as observed by Guidotti et al. and in this study, respectively. However at higher C-rates, the capacity values obtained in our study with XG were slightly lower than what was obtained by their study. At C/2, capacities of 220 mAh g⁻¹ and 180 mAh g⁻¹ were obtained by their and this study, respectively; and at C, capacities of 100 mAh g⁻¹ and 75 mAh g⁻¹ were obtained by their and this study, respectively. It seems that our MCMB provided lower C-rate capability. However, the purpose of this work was to show a comparative study of the capability of different alternative water-soluble binders.

As previously mentioned, XG is namely used as a thickener in salad dressing, where it makes the dressing foamy and viscous. It has the same effect when used in water with carbon; thus the slurry is foamier when compared with PVDF or CMCs, which makes the casting step more challenging. To prepare the slurry an aqueous solution of 1 wt% XG was used, as a more concentrated solution made the slurry solid-like. We investigated the fabrication of the films using a constant casting speed but different blade heights: 430 μm, 365 μm and 300 μm which represent the thicknesses of the wet films. Fig. 10 shows the cycling performance of the bat-
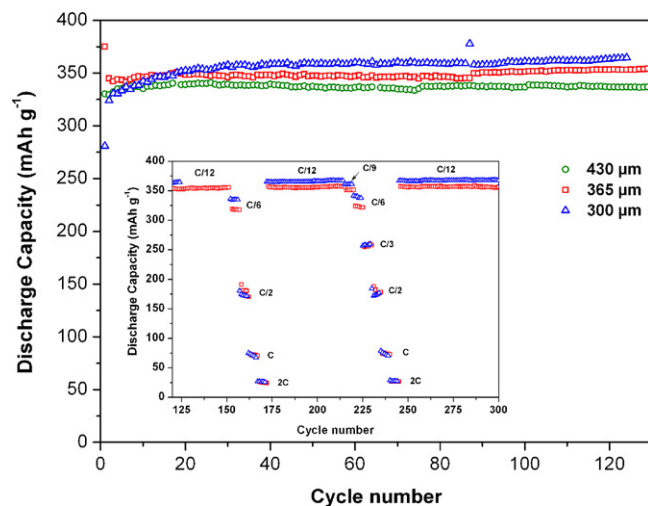

Fig. 10. Cycling behaviour of MCMB anodes prepared with XG using different film thicknesses. The batteries were cycled between 5 mV and 1.5 V versus Li/Li⁺ at C/12. The Inset is the cycling behaviour of MCMB anodes prepared with XG using two different film thicknesses, 365 and 300 μm. The batteries were cycled between 5 mV and 1.5 V versus Li/Li⁺ at different C-rates.

teries prepared with different anode thicknesses. The best results were obtained with thicknesses of 300 and 365 μm (thickness of the wet film). They showed capacities of 365 mAh g^{-1} and 350 mAh g^{-1} after 130 cycles, respectively. Thicker (430 μm) films showed lower capacity values, 335 mAh g^{-1} and 316 mAh g^{-1} after 130 cycles. The Inset in Fig. 10 shows the C-rate capability of the MCMB electrodes made with a 300 and a 365 μm blade thickness. These batteries exhibit very stable capacities even after two sets of high C-rates cycling. When the batteries were cycled back at C/12, almost 100% capacity retention is obtained.

4. Conclusions

In this study we reported the synthesis of LiCMC, where characterization confirmed the carboxymethyl function was successfully attached to the cellulose. We also demonstrated that environmentally friendly and water-soluble binders could easily replace the conventional PVDF binder. When considering the capacities obtained at C/12 after 100 cycles, the order of performance of the Li/MCMB half cells made using the different binders is: XG > PVDF > Baytron > NaCMC (Calbiochem) > LiCMC. In addition, XG also showed the best rate capability of all binders with a capacity of 180 mAh g^{-1} at C/2 and very good capacity retention after 300 cycles at various C-rates. However, in order to obtain quality performance with XG, care must be taken during the preparation of the cast for the anode.

Acknowledgments

References

[1] G.-A. Nazri, G. Pistoia, Lithium Batteries: Science and Technology, Kluwer Academic Publisher, Boston, Dordrecht, New York, London, 2004, p. 708.
[2] A. Hérold, Bull. Soc. Chim. Fr. 187 (1955) 999.
[3] D. Guerard, A. Herold, Comptes Rendus des Seances de l'Academie des Sciences Serie C: Sciences Chimiques 275 (11) (1972) 571–572.
[4] D. Guerard, A. Herold, Carbon 13 (4) (1975) 337–345.
[5] J.O. Besenhard, H.P. Fritz, J. Electroanal. Chem. 53 (2) (1974) 329–333.
[6] M. Armand, French Pat. No. 7832977 (1978).
[7] R.S. Treptow, J. Chem. Educ. 80 (9) (2003) 1015.
[8] X.Y. Song, K. Kinoshita, T.D. Tran, J. Electrochem. Soc. 143 (6) (1996) L120–L123.
[9] M. Winter, J.O. Besenhard, M.E. Spahr, P. Novák, Adv. Mater. 10 (10) (1998) 725–763.
[10] J. Li, R.B. Lewis, J.R. Dahn, Electrochem. Solid-State Lett. 10 (2) (2007) A17–A20.
[11] A. Du Pasquier, F. Disma, T. Bowmer, A.S. Gozdz, G. Amatucci, J.M. Tarascon, J. Electrochem. Soc. 145 (2) (1998) 472–477.
[12] H. Maleki, G. Deng, A. Anani, J. Howard, J. Electrochem. Soc. 146 (9) (1999) 3224–3229.
[13] H. Maleki, G. Deng, I. Kerzhner-Haller, A. Anani, J.N. Howard, J. Electrochem. Soc. 147 (12) (2000) 4470–4475.
[14] M. Gaberscek, M. Bele, J. Drofenik, R. Dominko, S. Pejovnik, Electrochem. Solid-State Lett. 3 (4) (2000) 171–173.
[15] G. Oskam, P.C. Searson, T.R. Jow, Electrochem. Solid-State Lett. 2 (12) (1999) 610–612.
[16] N. Ohta, T. Sogabe, K. Kuroda, Carbon 39 (9) (2001) 1434–1436.
[17] S.S. Zhang, T.R. Jow, J. Power Sources 109 (2) (2002) 422–426.
[18] M.W. Verbrugge, B.J. Koch, J. Electrochem. Soc. 150 (3) (2003) A374–A384.
[19] S.F. Lux, F. Schappacher, A. Balducci, S. Passerini, M. Winter, J. Electrochem. Soc. 157 (3) (2010) A320–A325.
[20] H. Buqa, M. Holzapfel, F. Krumeich, C. Veit, P. Novák, J. Power Sources 161 (1) (2006) 617–622.
[21] S.D. Beattie, D. Larcher, M. Morcrette, B. Simon, J.M. Tarascon, J. Electrochem. Soc. 155 (2) (2008) A158–A163.
[22] N.S. Hochgatterer, M.R. Schweiger, S. Koller, P.R. Raimann, T. Wohrle, C. Wurm, M. Winter, Electrochem. Solid-State Lett. 11 (5) (2008) A76–A80.
[23] W.-R. Liu, M.-H. Yang, H.-C. Wu, S.M. Chiao, N.-L. Wu, Electrochem. Solid-State Lett. 8 (2) (2005) A100–A103.
[24] G.T. Kim, S.S. Jeong, M. Joost, E. Rocca, M. Winter, S. Passerini, A. Balducci, J. Power Sources 196 (2011) 2187–2194.
[25] S.-L. Chou, J.-Z. Wang, C. Zhong, M.M. Rahman, H.-K. Liu, S.-X. Dou, Electrochim. Acta 54 (28) (2009) 7519–7524.
[26] G.D.O. Machado, A.M. Regiani, A. Pawlicka, Polimery 48 (4) (2003) 273–279.
[27] J. Kaloustian, A.M. Pauli, J. Pastor, J. Therm. Anal. Calorim. 48 (4) (1997) 791–804.
[28] J. Drofenik, M. Gaberscek, R. Dominko, F.W. Poulsen, M. Mogensen, S. Pejovnik, Jamnik, J. Electrochim. Acta 48 (7) (2003) 883–889.
[29] S.S. Zhang, K. Xu, T.R. Jow, J. Power Sources 138 (1–2) (2004) 226–231.
[30] J. Drofenik, M. Gaberscek, R. Dominko, M. Bele, S. Pejovnik, J. Power Sources 94 (1) (2001) 97–101.
[31] M. Yoshio, R.J. Brodd, A. Kozawa, Lithium-ion Batteries: Science and Technologies, Springer, New York, London, 2009, p. 452.
[32] S. Hossain, Y.-K. Kim, Y. Saleh, R. Loutfy, J. Power Sources 114 (2) (2003) 264–276.
[33] A. Sano, M. Kurihara, T. Abe, Z. Ogumi, J. Electrochem. Soc. 156 (8) (2009) A682–A687.
[34] H. Wang, T. Abe, S. Maruyama, Y. Iriyama, Z. Ogumi, K. Yoshikawa, Adv. Mater. 17 (23) (2005) 2857–2860.
[35] H.C. Starck, http://www.nanomechanics.pratt.duke.edu/MSDS/3%204_Polyethylenedioxythiopenepolystyrenesulfonate.pdf, Number PD-6002, Issue 2-05.09.2006.
[36] http://www.sigmaaldrich.com.
[37] A. Baar, W.-M. Kulicke, K. Szablikowski, R. Kiesewetter, Macromol. Chem. Phys. 195 (5) (1994) 1483–1492.
[38] P.B. Balbuena, Y. Wang, Lithium-ion Batteries: Solid–Electrolyte Interphase, Imperial College Press, London, 2004.
[39] H.J. Ahonen, J. Lukkari, J. Kankare, Macromolecules 33 (18) (2000) 6787–6793.
[40] J.-H. Lee, U. Paik, V.A. Hackley, Y.-M. Choi, J. Electrochem. Soc. 152 (9) (2005) A1763–A1769.
[41] R.A. Guidotti, F.W. Reinhardt, G. Sandi, Proceedings of the 39th Power Sources Conference, Cherry Hill, USA, June 12–15, 2000.